LRRK2 plays essential roles in maintaining lung homeostasis and preventing the development of pulmonary fibrosis

Yujie Tian[a,b,c,1], Jiaoyan Lv[a,c,1], Ziyan Su[a,c], Tao Wu[a,c], Xiaoguang Li[a,b,c], Xiaoyu Hu[a,c], Jianhong Zhang[a,c], and Li Wu[a,c,2]

[a]Institute for Immunology, Tsinghua-Peking Center for Life Sciences, School of Medicine, Tsinghua University, Beijing 100084, China; [b]Joint Graduate Program of Peking-Tsinghua-National Institute of Biological Sciences, School of Life Sciences, Tsinghua University, Beijing 100084, China; and [c]Beijing Key Laboratory for Immunological Research on Chronic Diseases, Beijing 100084, China

Edited by Carl F. Nathan, Weill Medical College of Cornell University, New York, NY, and approved July 23, 2021 (received for review April 13, 2021)

Perturbation of lung homeostasis is frequently associated with progressive and fatal respiratory diseases, such as pulmonary fibrosis. Leucine-rich repeat kinase 2 (LRRK2) is highly expressed in healthy lungs, but its functions in lung homeostasis and diseases remain elusive. Herein, we showed that LRRK2 expression was clearly reduced in mammalian fibrotic lungs, and LRRK2-deficient mice exhibited aggravated bleomycin-induced pulmonary fibrosis. Furthermore, we demonstrated that in bleomycin-treated mice, LRRK2 expression was dramatically decreased in alveolar type II epithelial (AT2) cells, and its deficiency resulted in profound dysfunction of AT2 cells, characterized by impaired autophagy and accelerated cellular senescence. Additionally, LRRK2-deficient AT2 cells showed a higher capacity of recruiting profibrotic macrophages via the CCL2/CCR2 signaling, leading to extensive macrophage-associated profibrotic responses and progressive pulmonary fibrosis. Taken together, our study demonstrates that LRRK2 plays a crucial role in preventing AT2 cell dysfunction and orchestrating the innate immune responses to protect against pulmonary fibrosis.

LRRK2 | lung homeostasis | pulmonary fibrosis | alveolar type II epithelial cells | immune response

Maintaining lung homeostasis requires coordinated interactions between cells within nonhematopoietic and hematopoietic compartments, and perturbed lung homeostasis leads to various severe lung diseases. Pulmonary fibrosis is a common pathogenetic feature and a final outcome of many lung diseases (1). Idiopathic pulmonary fibrosis (IPF) is a particularly common and fatal lung disease, characterized by excessive matrix deposition, destruction of normal lung architecture, and ultimately respiratory failure (2). Although the occurrence of IPF was suggested to be closely associated with disturbance of lung homeostasis and alterations in pulmonary function, its underlying cellular and molecular mechanisms remain unclear and urgently require in-depth investigation (3, 4).

Existing evidence suggests that alveolar epithelial cells play a crucial role in the maintenance of lung homeostasis and the pathogenesis of IPF (3, 5). Repeated alveolar epithelial microinjuries triggered by genetic or environmental factors are sufficient to initiate fibrotic progression (2, 3). Alveolar type II epithelial (AT2) cells can release various profibrotic cytokines or chemokines to recruit and activate immune cells, including monocyte-derived macrophages (mo-Macs) (6). In the progression of IPF, mo-Macs are skewed to become alternatively activated upon stimulation of Th2 cytokines such as IL-4 and IL-13 (7). Previous research has revealed that the alternatively activated macrophages (AAMs) were accumulated in both human and murine fibrotic lungs, and those AAMs facilitated the progression of pulmonary fibrosis via production of the profibrotic effectors (e.g., TGF-β1) and up-regulation of L-arginine metabolism by Arginase 1 (ARG1) (8).

Leucine-rich repeat kinase 2 (LRRK2) is a large protein containing a Ras of complex proteins (ROC) domain, a C-terminal of Roc domain, a leucine-rich repeat domain, and a kinase domain (9). LRRK2 is widely expressed in a variety of cells and involved in diverse processes such as neuronal plasticity, autophagy, and vesicle trafficking (10–13). Variants of *LRRK2* have been identified to be associated with increased risk of Parkinson's disease, Crohn's disease, and leprosy (14–16). Structural analysis has showed that LRRK2 evolutionally belongs to the receptor-interacting protein kinase (RIPK) family and is therefore also named RIPK7. Several members in the RIPK family have been identified to be critical regulators of cell death and innate immunity (17). The NOD/RIPK2 signaling pathway was reported to be essential for host defenses against lung infection (18) and RIPK3-regulated necroptosis in alveolar epithelial cells was involved in the pathogenesis of IPF (19). The previous studies reported that *Lrrk2*$^{-/-}$ mice exhibited alterations in AT2 cell morphology, implying a role of LRRK2 in lung physiology (20, 21). However, it remains elusive so far whether LRRK2 plays any important roles in regulating lung homeostasis or diseases.

In this study, we observed a clear down-regulation of LRRK2 expression in human and murine fibrotic lungs, which prompted us to further investigate the regulatory role of LRRK2 during the course of pulmonary fibrosis. Using the classical bleomycin-induced pulmonary fibrosis (BIPF) mouse model, we found that LRRK2-deficient mice displayed more rapid and exacerbated fibrotic

Significance

Pulmonary fibrosis is a common final outcome of many lung diseases, and its occurrence may be closely associated with the disturbance of lung homeostasis and with alterations in pulmonary function. In this study, we identified leucine-rich repeat kinase 2 (LRRK2) as a pivotal molecule in alveolar type II epithelial (AT2)–coordinated pulmonary responses in the context of bleomycin-induced pulmonary fibrosis. Our results demonstrated that LRRK2 restrained progressive pulmonary fibrosis by preventing AT2 cell dysfunction and the subsequent CCL2/CCR2 axis–dependent macrophage-mediated profibrotic responses. Our study highlights the important biological functions of LRRK2 in the maintenance of lung homeostasis and the prevention of fibrotic lung disease, thereby providing a potential target for developing clinical therapeutic strategies.

Author contributions: Y.T., J.L., and L.W. designed research; Y.T., J.L., and Z.S. performed research; X.L. and J.Z. contributed new reagents/analytic tools; Y.T., J.L., and Z.S. analyzed data; and Y.T., J.L., T.W., X.H., and L.W. wrote the paper.

The authors declare no competing interest.

This article is a PNAS Direct Submission.

[1]Y.T. and J.L. contributed equally to this work.

[2]To whom correspondence may be addressed. Email: wuli@mail.tsinghua.edu.cn.

This article contains supporting information online at https://www.pnas.org/lookup/suppl/doi:10.1073/pnas.2106685118/-/DCSupplemental.

Published August 26, 2021.

progression, accompanied by extensive macrophage-mediated profibrotic immune responses after bleomycin insult. We further demonstrated that LRRK2-deficient AT2 cells exhibited impaired autophagy and accelerated cellular senescence, which led to increased chemokine production and the subsequent infiltration of macrophages and aggravated profibrotic responses. Together, our findings revealed a critical role for LRRK2 in maintaining the AT2 cell function and preventing the development of pulmonary fibrosis.

Results

LRRK2 Expression Was Down-regulated in Fibrotic Lungs and Its Deficiency in Mice Exacerbated Pulmonary Fibrosis. To determine whether the expression of *Lrrk2* was dysregulated during pulmonary fibrosis, we firstly challenged wild-type (WT) C57BL/6 mice with bleomycin, the most widely used and best-characterized agent for studying murine pulmonary fibrosis (22). Similar to the expression profiles in human (*SI Appendix*, Fig. S1 *A* and *B*), *Lrrk2* exhibited markedly higher expression in murine lungs than most other tissues in homeostatic condition according to the published databases (*SI Appendix*, Fig. S1 *C* and *D*). However, the messenger RNA (mRNA) and protein levels of *Lrrk2* were significantly decreased in lung tissues isolated from bleomycin-treated mice 10 d after instillation compared with those in saline-treated mice (Fig. 1 *A* and *B*), suggesting a dynamic regulation of LRRK2 during the progression of pulmonary fibrosis.

To evaluate the effects of LRRK2 loss on the pathogenesis of pulmonary fibrosis in vivo, we administrated bleomycin to the LRRK2-deficient ($Lrrk2^{-/-}$) and WT mice and killed the mice 10

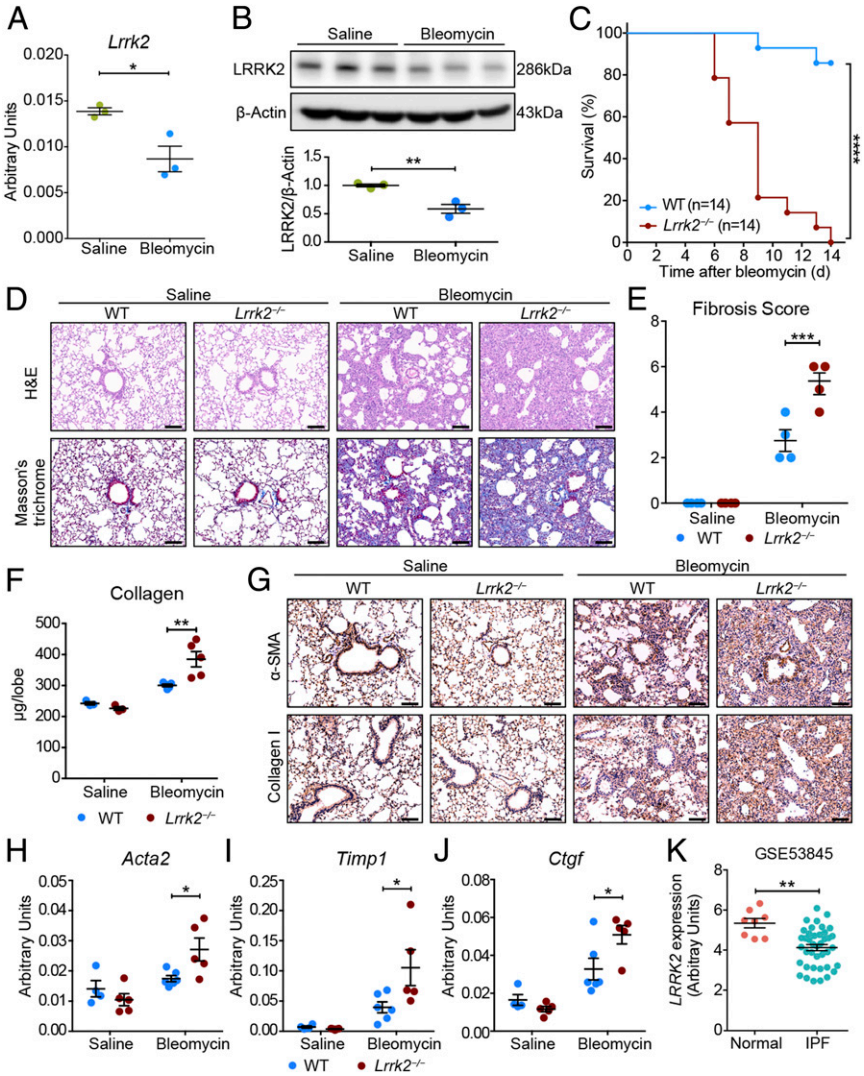

Fig. 1. LRRK2 expression was down-regulated in fibrotic lungs, and its deficiency in mice exacerbated pulmonary fibrosis. (*A* and *B*) Quantitative analyses of (*A*) *Lrrk2* mRNA by qRT-PCR and (*B*) LRRK2 protein by Western blot in lung tissues of WT male mice after saline or 1.5 mg/kg bleomycin treatment for 10 d (n = 3 mice per group). (*C*) Survival curves of bleomycin-treated WT and $Lrrk2^{-/-}$ male mice were recorded over a 14-d period (n = 14 mice per group); ****P < 0.0001, by log-rank test. (*D–J*) WT and $Lrrk2^{-/-}$ male mice were challenged with saline or bleomycin for 10 d (n = 3 to 6 mice per group). (*D*) Representative images of the H&E- and Masson's trichrome–stained lung sections. (Scale bars: 100 μm.) (*E*) Fibrosis score based on stained lung sections from saline or bleomycin-treated groups. (*F*) Quantification of collagen content in lung homogenates using the Sircol Assay. (*G*) Representative immunohistochemical analysis of α-SMA and Collagen I in lung sections. (Scale bars: 100 μm.) Quantitative analyses of mRNA expression of indicated profibrotic genes including (*H*) *Acta2*, (*I*) *Timp1*, and (*J*) *Ctgf* in lung tissues by qRT-PCR. (*K*) *LRRK2* mRNA expression in lung samples of IPF patients (n = 40) compared with normal controls (n = 8) based on the reanalysis of a published dataset (GSE53845) (24). Data in *A*, *B*, *E*, *F*, and *H–J* are representative of two to three independent experiments. Data are shown as mean ± SEM; *P < 0.05, **P < 0.01, ***P < 0.001 by two-tailed Student's t test (*A*, *B*, *K*) and two-way ANOVA followed by Bonferroni's multiple comparisons test (*E*, *F*, *H–J*).

or 14 d postinstillation. The *Lrrk2*$^{-/-}$ mice displayed enhanced susceptibility to bleomycin challenge with a significantly higher mortality rate (Fig. 1*C*). As shown by the results of hematoxylin and eosin (H&E) and Masson's trichrome staining of lung sections, both saline-instilled WT and *Lrrk2*$^{-/-}$ mice exhibited no fibrotic burden (Fig. 1*D*). In contrast, for the bleomycin-treated groups, *Lrrk2*$^{-/-}$ mice developed significantly exacerbated pulmonary fibrosis, as evidenced by severe disruption of lung structure and augmented collagen deposition, compared with WT mice 10 d after bleomycin exposure (Fig. 1*D*). The degree of fibrotic lesions in *Lrrk2*$^{-/-}$ mice at day 10 was comparable to that of WT mice at day 21, indicating an accelerated progression of pulmonary fibrosis (Fig.1*D* and *SI Appendix*, Fig. S2*A*). Consistently, the Ashcroft fibrosis score (23) on histology and collagen contents in lung were also elevated in the lungs of bleomycin-treated *Lrrk2*$^{-/-}$ mice (Fig. 1 *E* and *F*). In line with that, the results of microcomputed tomography analysis showed a markedly increased lung density in bleomycin-treated *Lrrk2*$^{-/-}$ mice (*SI Appendix*, Fig. S2*B*). The bleomycin-treated *Lrrk2*$^{-/-}$ mice also displayed impaired pulmonary function, revealed by significantly higher lung resistance (RL) and lower dynamic lung compliance (Cdyn) and minute ventilation volume (MV) (*SI Appendix*, Fig. S2*C*). In addition, immunohistochemical staining showed increased depositions of α-SMA and Collagen I, markers reflecting the accumulation and activation of myofibroblasts, in lung of bleomycin-treated *Lrrk2*$^{-/-}$ mice (Fig. 1*G*). Furthermore, the bleomycin-induced expression of fibrosis-associated genes, including *Acta2*, *Timp1*, and *Ctgf*, were also significantly up-regulated in the lungs of *Lrrk2*$^{-/-}$ mice (Fig. 1 *H–J*), clearly demonstrating exacerbated BIPF caused by LRRK2 deficiency.

In line with the observations in mice (Fig. 1*A*), reanalysis of a published gene expression microarray dataset of human IPF lungs (24) also identified a significant decrease in the mRNA expression of *LRRK2* in human IPF lung tissues compared with the normal control group ($log_2FC = -1.3$; Fig. 1*K*). The bleomycin-treated LRRK2-deficient mice and those IPF patients displayed similar pulmonary dysfunction and fibrotic progression. Thus, LRRK2 may play an indispensable protective role in the progression of both murine BIPF and human IPF.

LRRK2 Deficiency Led to Enhanced Bleomycin-Elicited Profibrotic Immune Responses. Bleomycin-induced fibrotic progression is usually initiated by inflammatory reactions within a short period (25). Therefore, we examined whether LRRK2 played a regulatory role in bleomycin-induced lung inflammation. As shown in the H&E staining of lung sections (Fig. 2*A*), only resident alveolar macrophages (blue arrow) were observed in the alveolar spaces of both WT and *Lrrk2*$^{-/-}$ mice in the saline-treated groups. In contrast, significantly increased infiltrating cells could be detected in the alveolar spaces of both WT and *Lrrk2*$^{-/-}$ mice 7 d after bleomycin treatment, with more infiltrating neutrophils (black arrows) in the alveoli and interstitium of *Lrrk2*$^{-/-}$ mice than that of WT mice (Fig. 2*A*). To further investigate the immune cell profile, we applied the gating strategy modified from a previous study (26) to identify myeloid cell subsets and lymphocytes in the lungs of saline- or bleomycin-treated WT and *Lrrk2*$^{-/-}$ mice (*SI Appendix*, Fig. S3 *A* and *B*). In the saline-treated group, both WT and *Lrrk2*$^{-/-}$ mice displayed comparable numbers in each immune cell subpopulation, suggesting that LRRK2 was dispensable for maintaining the proper immune cell compositions in lung tissues at steady state (Fig. 2*B* and *SI Appendix*, Fig. S3*C*). It is noteworthy that the numbers of lung CD11b^{+}F4/80^{+} mo-Macs and CD11b^{+}Ly6G^{+} neutrophils in bleomycin-treated *Lrrk2*$^{-/-}$ mice were significantly higher than those in WT control mice (Fig. 2*B* and *SI Appendix*, Fig. S3*A*). After bleomycin treatment, the numbers of lung-infiltrating dendritic cells and B cells were lower in *Lrrk2*$^{-/-}$ mice (*SI Appendix*, Fig. S3*C*).

We further measured the production of several major cytokines and chemokines in bronchoalveolar lavage fluid (BALF) and lungs collected from WT and *Lrrk2*$^{-/-}$ mice 7 d after bleomycin instillation. Although upon bleomycin treatment, comparable levels of total protein were detected in the BALF of WT and *Lrrk2*$^{-/-}$ mice (*SI Appendix*, Fig. S4*A*), significantly higher protein levels of active TGF-β1 and IL-6 could be seen in the BALF of *Lrrk2*$^{-/-}$ mice (Fig. 2 *C* and *D*). In addition, up-regulated protein levels of monocyte/macrophage chemoattractant CCL2 and neutrophil chemoattractant CXCL1 were also observed in the BALF of *Lrrk2*$^{-/-}$ mice after bleomycin instillation (Fig. 2 *E* and *F*), which correlated with the increased infiltration of mo-Macs and neutrophils in lung (Fig. 2*B*). Furthermore, a significantly higher protein level of IL-13, but not IFNγ or IL-17A, was detected in lung homogenates of bleomycin-treated *Lrrk2*$^{-/-}$ mice compared with that from WT control mice (*SI Appendix*, Fig. S4 *B–D*). As TGF-β1, IL-6, and IL-13 are all critical profibrotic cytokines in promoting pulmonary fibrosis (27–30), the results described indicated that LRRK2 deficiency led to markedly elevated production of profibrotic mediators and enhanced profibrotic immune responses in BIPF.

LRRK2 Deficiency Promoted the Profibrotic Polarization of mo-Macs in BIPF. During the disease progression of murine BIPF and human IPF, macrophages differentiated from circulating monocytes can be polarized to either a proinflammatory or profibrotic phenotype, thereby acting as a central regulator of pulmonary fibrosis (31, 32). Since we have observed a significant increase in the number of mo-Macs in the lung of bleomycin-treated *Lrrk2*$^{-/-}$ mice (Fig. 2*B*), we wished to investigate whether the exacerbated pulmonary fibrosis is associated with polarization of these macrophages to a profibrotic phenotype. We purified the mo-Macs from the lungs of saline- or bleomycin-treated WT and *Lrrk2*$^{-/-}$ mice (*SI Appendix*, Fig. S5*A*) and evaluated the mRNA expressions of macrophage activation markers. Importantly, mo-Macs from bleomycin-treated *Lrrk2*$^{-/-}$ mice displayed a significant higher expression of the alternative macrophage activation hallmark genes *Chil3* and *Arg1* (Fig. 2 *G* and *H*), but not classically activated macrophage markers *Tnf*, *Il6*, and *Il1b* (*SI Appendix*, Fig. S5 *B–D*), compared with WT control group. In addition, mo-Macs isolated from bleomycin-treated *Lrrk2*$^{-/-}$ mice also produced significantly higher levels of profibrotic factors *Spp1* and *S100a4* (Fig. 2 *I* and *J*), which were identified as critical factors for promoting the differentiation and survival of lung fibroblasts in the progression of pulmonary fibrosis (33–35).

To determine whether LRRK2 regulates macrophage polarization in a cell-intrinsic manner, we generated bone marrow-derived macrophages (BMDMs) from WT and *Lrrk2*$^{-/-}$ mice and induced their classical and alternative activation, respectively. Consistent with previous studies (36, 37), LRRK2 deficiency did not affect the lipopolysaccharide (LPS)-induced up-regulation of *Tnf*, *Il6*, and *Il1b,* the hallmarks of classically activated macrophages (*SI Appendix*, Fig. S6 *A–C*). However, LPS cooperated with GM-CSF and IFNγ could induce higher *Il6* and *Il1b* production in *Lrrk2*$^{-/-}$ BMDMs (*SI Appendix*, Fig. S6 *B* and *C*). Surprisingly, we found that LRRK2 deficiency failed to enhance the alternative macrophage activation in response to IL-4 or the combination of IL-4 and M-CSF, as evidenced by similar levels of *Chil3*, *Retnla*, and *Arg1* compared with that in WT BMDMs (*SI Appendix*, Fig. S6 *D–F*). Therefore, LRRK2 deficiency seemed to skew the lung-infiltrating mo-Macs to a profibrotic phenotype by creating a profibrotic lung microenvironment for them rather than in a cell-intrinsic manner during the progression of pulmonary fibrosis.

LRRK2 Deficiency in Nonhematopoietic Cells Served as the Major Contributor to the Exacerbation of Pulmonary Fibrosis. To assess the relative contribution of hematopoietic and nonhematopoietic cells to the BIPF exacerbation in *Lrrk2*$^{-/-}$ mice, we utilized reciprocal bone marrow (BM) transplantation and generated the following chimeric mice: WT → WT, *Lrrk2*$^{-/-}$ → WT, WT → *Lrrk2*$^{-/-}$, and *Lrrk2*$^{-/-}$ → *Lrrk2*$^{-/-}$ (Fig. 3*A*). At 6 wk after BM transplantation,

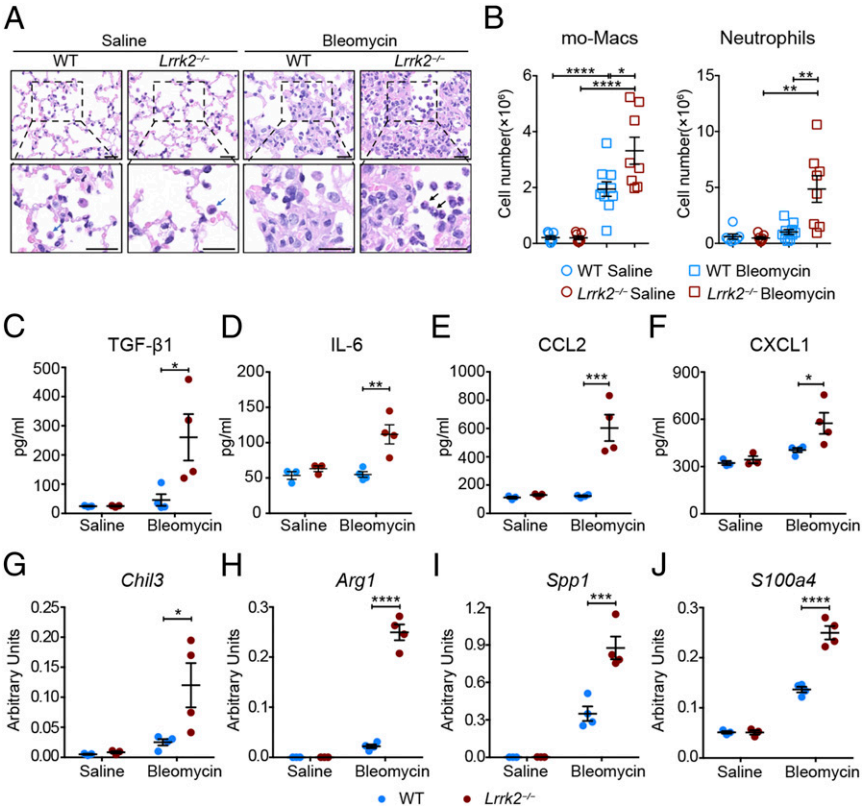

Fig. 2. LRRK2 deficiency led to enhanced profibrotic immune responses and promoted the profibrotic polarization of mo-Macs in the development of pulmonary fibrosis. WT and *Lrrk2*$^{-/-}$ male mice were challenged with saline or 1.5 mg/kg bleomycin for 7 d. (*A*) Representative images of H&E-stained lung sections; blue arrow: alveolar macrophage; black arrow: neutrophil. (Scale bars: 20 μm.) (*B*) Flow cytometric analysis and quantification of mo-Macs and neutrophils in enzymatically digested whole lung tissues from saline- or bleomycin-treated WT and *Lrrk2*$^{-/-}$ mice (n = 7 to 10 mice per group). (*C–F*) ELISA analysis of (*C*) TGF-β1, (*D*) IL-6, (*E*) CCL2, and (*F*) CXCL1 levels in BALF from WT and *Lrrk2*$^{-/-}$ mice (n = 3 to 4 mice per group). (*G–J*) Quantification of mRNA levels of profibrotic factors, including (*G*) *Chil3*, (*H*) *Arg1*, (*I*) *Spp1*, and (*J*) *S100a4*, by qRT-PCR in isolated lung mo-Macs (n = 3 to 4 mice per group). Data are shown as mean ± SEM and are (*B*) integrated from three independent experiments or (*C–J*) representative of three independent experiments. *P < 0.05, **P < 0.01, ***P < 0.001, ****P < 0.0001, by (*B*) two-tailed Student's t test or (*C–J*) two-way ANOVA followed by Bonferroni's multiple comparison test.

mice were subjected to bleomycin exposure. During a 14-d experimental period, we found that mice with LRRK2 deficiency in nonhematopoietic compartment (WT → *Lrrk2*$^{-/-}$ and *Lrrk2*$^{-/-}$ → *Lrrk2*$^{-/-}$) suffered from significantly higher bleomycin-induced mortality rates (Fig. 3*B*). Histologically, mice with WT nonhematopoietic cells (WT → WT and *Lrrk2*$^{-/-}$ → WT) still maintained a large amount of normal lung architecture and only exhibited mild lung fibrosis after intratracheal bleomycin challenge (Fig. 3*C*). In contrast, mice with *Lrrk2*$^{-/-}$ nonhematopoietic cells (WT → *Lrrk2*$^{-/-}$ and *Lrrk2*$^{-/-}$ → *Lrrk2*$^{-/-}$) displayed extensive destruction of lung architecture and prominent fibrotic lesions, corroborated by more excessive collagen deposition and higher Ashcroft fibrosis scores in response to bleomycin (Fig. 3 *C* and *D*). Apart from significantly elevated collagen contents (Fig. 3*E*), induction of typical fibrosis-associated genes *Acta2*, *Timp1*, and *Ctgf* were also significantly enhanced in lung tissues resulted from LRRK2 deficiency in nonhematopoietic cells (WT → *Lrrk2*$^{-/-}$ and *Lrrk2*$^{-/-}$ → *Lrrk2*$^{-/-}$) at 10 d after bleomycin treatment (Fig. 3 *F–H*). Thus, these data suggested that LRRK2 deficiency in nonhematopoietic cells, but not in BM-derived cells, exacerbated bleomycin-elicited lethality and fibrotic processes.

We next went to uncover how LRRK2 deficiency in nonhematopoietic cells contributed to the development of pulmonary fibrosis. We found that mice with LRRK2 deficiency in nonhematopoietic cells (WT → *Lrrk2*$^{-/-}$ and *Lrrk2*$^{-/-}$ → *Lrrk2*$^{-/-}$) exhibited significantly enhanced production of profibrotic cytokine TGF-β1 in BALF after bleomycin treatment (Fig. 4*A*). Similar to the observations in Fig. 2*B*, the numbers of lung-infiltrating mo-Macs were significantly increased in bleomycin-treated mice from WT → *Lrrk2*$^{-/-}$ and *Lrrk2*$^{-/-}$ → *Lrrk2*$^{-/-}$ groups compared to those in WT → WT and *Lrrk2*$^{-/-}$ → WT groups (Fig. 4*B*). Meanwhile, LRRK2 deficiency in the nonhematopoietic compartment (WT → *Lrrk2*$^{-/-}$ and *Lrrk2*$^{-/-}$ → *Lrrk2*$^{-/-}$) was responsible for the higher levels of CXCL1 and increased numbers of lung-infiltrating neutrophils upon bleomycin exposure (Fig. 4*C* and *SI Appendix*, Fig. S7 *A* and *B*). Furthermore, LRRK2 deficiency in nonhematopoietic cells (WT → *Lrrk2*$^{-/-}$ and *Lrrk2*$^{-/-}$ → *Lrrk2*$^{-/-}$) contributed to the polarization of mo-Macs to a profibrotic phenotype rather than a proinflammatory phenotype, characterized by significantly elevated induction of profibrotic genes *Chil3*, *Arg1*, and *Spp1* (Fig. 4 *D–F* and *SI Appendix*, Fig. S7 *C–E*). Collectively, our results illustrated that the alterations of nonhematopoietic cells caused by LRRK2 deficiency created a profibrotic lung environment to facilitate the infiltration of key profibrotic myeloid immune cells and the profibrotic polarization of mo-Macs, thereby serving as the major contributor to the exacerbated BIPF.

Down-regulation of LRRK2 in AT2 Cells Is Closely Associated with the Progression of Pulmonary Fibrosis. To pinpoint the target cell types of LRRK2 deficiency, we firstly evaluated LRRK2 expression levels in each lung-resident cell type, especially in the nonhematopoietic compartment. By mining a recently published human lung single-cell RNA-sequencing dataset (38), we found that *LRRK2* was predominantly expressed by AT2 cells, which were regarded as the key nonhematopoietic cells involved in IPF pathogenesis (2)

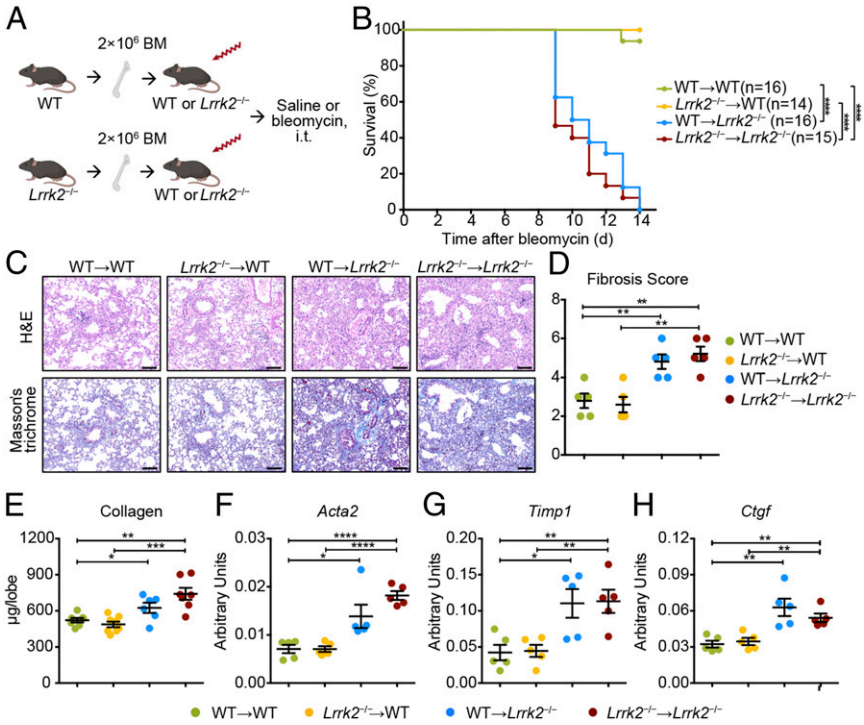

Fig. 3. LRRK2 deficiency in nonhematopoietic cells accounted for the enhanced severity to bleomycin-mediated fibrosis. (*A*) Scheme of BM chimeric mice construction and experimental design. Icons were created with BioRender.com. (*B*) Survival curves of mice from the four groups of BM chimeric mice treated with 1.5 mg/kg bleomycin (n = 14 to 16 mice per group) were recorded over a 14-d period; ****$P < 0.0001$ by log-rank test. (*C–H*) Lung tissues from bleomycin-treated BM chimeric mice (n = 5 to 6 mice per group) were harvested at day 10 for the following analyses. (*C*) Representative images of H&E- and Masson's trichrome–stained lung tissue sections. (Scale bars: 100 μm.) (*D*) Fibrosis scores based on stained lung sections. (*E*) Quantification of collagen content in lung homogenates using the Sircol Assay. Quantitative analyses of mRNA levels of indicated fibrosis-associated genes, including (*F*) *Acta2*, (*G*) *Timp1*, and (*H*) *Ctgf*, by qRT-PCR in lung tissues from indicated BM chimeric mice after bleomycin challenge. Data in *D–H* are shown as mean ± SEM and are representative of three independent experiments. *$P < 0.05$, **$P < 0.01$, ***$P < 0.001$, ****$P < 0.0001$, by two-tailed Student's t test.

among all characterized cell types in the human respiratory tree (*SI Appendix*, Fig. S8*A*). Consistently, murine AT2 cells also harbored the highest *Lrrk2* expression among all cellular components in lung (*SI Appendix*, Fig. S8*B*), which is in line with an essential role of *Lrrk2* for AT2 homeostasis or function. Similar to the morphological alterations reported by previous studies (20, 21), we also observed an accumulation of enlarged lamellar bodies in AT2 cells of *Lrrk2*$^{-/-}$ mice compared with WT mice (*SI Appendix*, Fig. S9 *A–D*). Furthermore, AT2 cells in *Lrrk2*$^{-/-}$ mice exhibited an enhancement of autofluorescence and an up-regulation of characteristic lamellar body-associated genes, such as cathepsins and V-ATPases (39) (*SI Appendix*, Fig. S9 *E* and *F*), indicating an alteration in their homeostasis.

Next, we reanalyzed published bulk and single-cell transcriptomic datasets of AT2 cells isolated from healthy individuals or IPF patients (40) and observed that *LRRK2* expression was significantly decreased in AT2 cells from human IPF patients compared with healthy controls (Fig. 5 *A* and *B*). Similar to the pattern of LRRK2 expression in AT2 cells from IPF patients, AT2 cells isolated from bleomycin-treated WT mice also showed dramatically decreased expression of LRRK2 protein (Fig. 5*C*). Meanwhile, LRRK2 was minimally expressed in lung fibroblasts and dispensable for their activation in response to TGF-β in vitro (*SI Appendix*, Fig. S8 and S10). Thus, these results prompted us that insufficient expression of LRRK2 in AT2 cells was closely associated with the progression of pulmonary fibrosis and LRRK2 could exert regulatory effect directly on the function of AT2 cells.

LRRK2 Deficiency Led to Profound Dysfunction of AT2 Cells in the Context of Pulmonary Fibrosis. As LRRK2 deficiency did not affect the magnitude of AT2 cell either in naïve or fibrotic mice (*SI Appendix*, Fig. S11), we next investigated the mechanisms by which LRRK2 regulated the function of AT2 cells in the pathogenesis of pulmonary fibrosis. The aberrant exacerbation of BIPF caused by LRRK2 deficiency could be related to an accompanying defective autophagy because the latter has been shown to contribute to pulmonary fibrosis by inducing AT2 cell dysfunction (41, 42). To address this question, we assessed autophagic activity in AT2 cells from both WT and *Lrrk2*$^{-/-}$ mice after saline or bleomycin administration. Immunohistochemical staining and Western blot analysis showed that AT2 cells from bleomycin-treated *Lrrk2*$^{-/-}$ mice exhibited markedly elevated accumulation of p62, a selective substrate of autophagic degradation (43), compared to WT control mice (Fig. 5 *D* and *E*). To further monitor the autophagic flux, we utilized Western blot to detect the abundance of LC3B-II, which reflects the autophagosome formation (43), in isolated AT2 cells. The results illustrated impaired conversion from LC3B-I to LC3B-II in AT2 cells from bleomycin-treated *Lrrk2*$^{-/-}$ mice compared to that in WT mice (Fig. 5*E*). In addition, ultrastructural analyses of AT2 cells revealed that the formation of autophagic vacuoles was readily observed in WT AT2 cells but barely visible in *Lrrk2*$^{-/-}$ AT2 cells after bleomycin exposure (Fig. 5*F*). Expression of ATG16L1, which plays an essential role in autophagosome formation through interacting with ATG12-ATG5 to mediate the transition of LC3-I to LC3-II (44), was also significantly down-regulated in AT2 cells from bleomycin-treated *Lrrk2*$^{-/-}$ mice (Fig. 5*G*). We further examined the signaling pathways upstream of autophagy that can be regulated by LRRK2 (45–48). Western blot results showed that LRRK2 deficiency led to dramatic attenuation in ERK activation in AT2 cells at steady state and in the progression of pulmonary fibrosis (Fig. 5*H*). The activation of JNK signaling pathway was also down-regulated to some

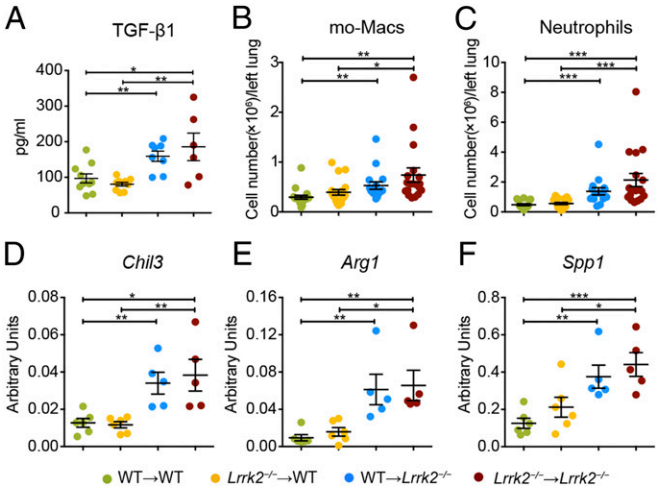

Fig. 4. LRRK2 deficiency in nonhematopoietic cells promoted profibrotic immune responses and the profibrotic polarization of mo-Macs upon bleomycin exposure. The four groups of BM chimeric mice were challenged with 1.5 mg/kg bleomycin for 7 d. (*A*) TGF-β1 expression in BALF were quantified by ELISA analysis ($n = 6$ to 10 mice per group). (*B* and *C*) Numbers of (*B*) mo-Macs and (*C*) neutrophils in lung tissues were quantified by flow cytometry ($n = 16$ to 19 mice per group). (*D–F*) Quantification of relative mRNA levels of profibrotic factors including (*D*) *Chil3*, (*E*) *Arg1*, and (*F*) *Spp1* by qRT-PCR in isolated lung mo-Macs ($n = 5$ to 6 mice per group). Data are shown as mean ± SEM and are (*A–C*) integrated from or (*D–F*) representative of at least two independent experiments. $^*P < 0.05$, $^{**}P < 0.01$, $^{***}P < 0.001$, by two-tailed Student's *t* test.

extent after bleomycin treatment, while the activation of mTOR and Wnt/β-catenin signaling pathways were not affected by LRRK2 deletion (Fig. 5*H*). These results collectively indicated that LRRK2 deficiency led to impaired autophagy of AT2 cells during the pathogenesis of BIPF.

Insufficient autophagy has been proposed to contribute to accelerated cellular senescence of airway epithelial cells, a major feature implicated in IPF pathogenesis (49). We next investigated whether impaired autophagy could drive cellular senescence in LRRK2-deficient AT2 cells after bleomycin treatment. Western blot analysis showed a significantly elevated induction of p53 and p21 proteins, the central effectors involved in cell injury and senescence (50, 51), in AT2 cells from bleomycin-treated *Lrrk2*$^{-/-}$ mice compared to those in WT mice (Fig. 6*A*). Senescent cells elicit chronic inflammation through secreting cytokines, chemokines, and proteases, termed the senescence-associated secretory phenotype (SASP) (52). We further evaluated the expression of canonical SASP factors CCL2 and IL-6 (52) in isolated AT2 cells, and markedly increased transcript levels of Ccl2 and Il6 were observed in *Lrrk2*$^{-/-}$ AT2 cells compared with that of WT AT2 cells upon bleomycin exposure (Fig. 6 *B* and *C*). This change was consistent with the elevated protein levels of *CCL2* and *IL-6* in BALF harvested from bleomycin-treated *Lrrk2*$^{-/-}$ mice (Fig. 2 *D* and *E*) and associated with the phenotype of increased infiltration of mo-Macs and neutrophils in lung tissues of bleomycin-treated *Lrrk2*$^{-/-}$ mice (Fig. 2*B*). In addition, AT2 cells isolated from bleomycin-treated *Lrrk2*$^{-/-}$ mice also exhibited prominent up-regulation of SASP factors *Serpine1*, *Mmp2*, and *Mmp10* (Fig. 6 *D–F*). Together, these results indicated that loss of LRRK2 led to autophagic defects and accelerated cellular senescence in AT2 cells, thereby mediating enhanced recruitment of infiltrating profibrotic immune cells in the context of bleomycin-driven pulmonary fibrosis.

The Enhanced Recruitment of mo-Macs and Aberrant Profibrotic Responses Were CCL2/CCR2 Dependent in LRRK2-Deficient Mice. Our results suggested that the increased number of infiltrating profibrotic mo-Macs in bleomycin-treated *Lrrk2*$^{-/-}$ mice was mediated by the elevated CCL2 production by AT2 cells (Figs. 2 *B* and *E* and 6*B*). BM chimeric experiments also supported this notion by showing that the increased levels of CCL2 in BALF were predominantly from *Lrrk2*$^{-/-}$ nonhematopoietic cells (Fig. 7*A*). CCR2 is known to be the sole receptor for CCL2 (53) and thus mediates macrophage migration in BIPF (54). To assess whether blocking the recruitment of mo-Macs into the lung could protect *Lrrk2*$^{-/-}$ mice from aggravated pulmonary fibrosis, we crossed *Ccr2*$^{-/-}$ mice with *Lrrk2*$^{-/-}$ mice to generate *Ccr2*$^{-/-}$*Lrrk2*$^{-/-}$ mice. Upon bleomycin challenge, reduced infiltration of mo-Macs and decreased expression of active

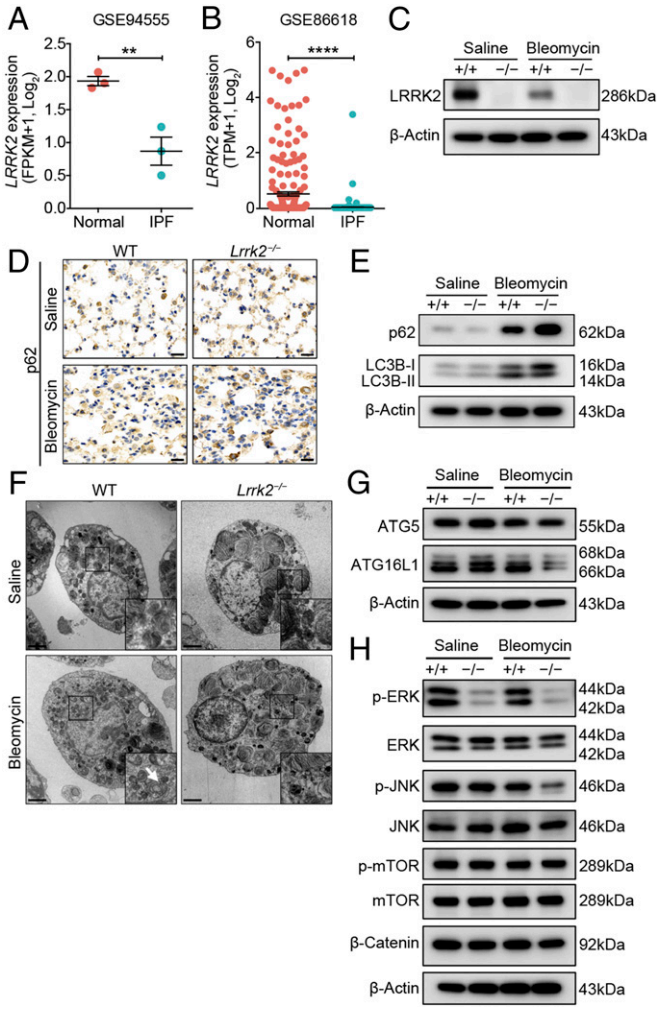

Fig. 5. LRRK2 expression was down-regulated, and its deficiency led to impaired autophagy in AT2 cells in the progression of pulmonary fibrosis. (*A* and *B*) *LRRK2* expression in AT2 cells from normal and IPF human lung tissues was determined based on published datasets (*A*) GSE94555 and (*B*) GSE86618 and displayed in dot plots. WT and *Lrrk2*$^{-/-}$ mice were treated with saline or 1.2 mg/kg bleomycin for 7 d ($n = 3$ to 4 mice per group). (*C*) Representative Western blot of LRRK2 expression in isolated AT2 cells. (*D*) Representative immunohistochemical analysis of p62 in lung sections. (Scale bars: 20 μm.) (*E*) Representative Western blot of p62, LC3B-I, and LC3B-II expression in isolated AT2 cells. (*F*) AT2 cells isolated from WT and LRRK2-deficient mice were evaluated by transmission electronic microscopy (original magnification: 4,200×). (Scale bars: 2 μm.) Magnified images of the boxed areas. The arrows indicate the autophagic vacuoles formed in bleomycin-treated WT mice. (*G*) Representative Western blot of ATG5 and ATG16L1 expression in isolated AT2 cells. (*H*) Representative Western blot of p-ERK, ERK, p-JNK, JNK, p-mTOR, mTOR, and β-Catenin expression in isolated AT2 cells. Three independent experiments were performed, and β-Actin was used as the loading control. Data are shown as mean ± SEM; $^{**}P < 0.01$, $^{****}P < 0.0001$, by two-tailed Student's *t* test (*A* and *B*).

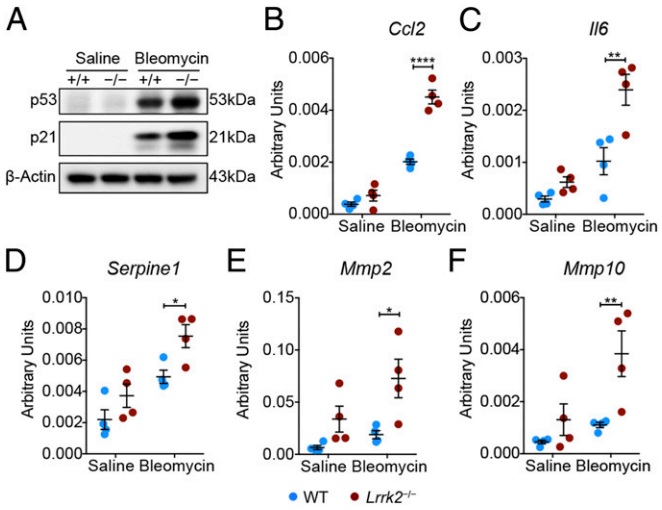

Fig. 6. LRRK2 deficiency led to increased cellular senescence in AT2 cells in the context of pulmonary fibrosis. WT and *Lrrk2*$^{-/-}$ mice were treated with saline or 1.2 mg/kg bleomycin for 7 d (n = 3 to 4 mice per group). (*A*) Representative Western blot of p53 and p21 expression in isolated AT2 cells. (*B–F*) Quantification of relative mRNA levels of representative SASP factors, including (*B*) *Ccl2*, (*C*) *Il6*, (*D*) *Serpine1*, (*E*) *Mmp2*, and (*F*) *Mmp10*, in isolated AT2 cells by qRT-PCR. Three independent experiments were performed, and β-Actin was used as the loading control. Data are shown as mean ± SEM; *P < 0.05, **P < 0.01, ****P < 0.0001, by two-way ANOVA followed by Bonferroni's multiple comparison test (*B–F*).

TGF-β1 were observed in *Ccr2*$^{-/-}$*Lrrk2*$^{-/-}$ mice compared to that from *Lrrk2*$^{-/-}$ mice (Fig. 7 *B* and *C*). Moreover, lung histological analysis clearly revealed attenuated distortion of lung architecture and reduced collagen deposition in *Ccr2*$^{-/-}$*Lrrk2*$^{-/-}$ mice compared to that in *Lrrk2*$^{-/-}$ mice after bleomycin insult (Fig. 7*D*). These results were corroborated by the significantly decreased levels of collagen contents in the lungs from *Ccr2*$^{-/-}$*Lrrk2*$^{-/-}$ mice (Fig. 7*E*). We also observed similar results through constructing BM chimeric mice by using *Ccr2*$^{-/-}$ mice as BM donors (*SI Appendix*, Fig. S12). Notably, although the number of neutrophils infiltrating the lungs of *Ccr2*$^{-/-}$*Lrrk2*$^{-/-}$ mice and the level of neutrophil chemoattractant CXCL1 were significantly lower than that of *Lrrk2*$^{-/-}$ mice, they were still significantly higher than that of *Ccr2*$^{-/-}$ mice (Fig. 7 *F–H*), suggesting that LRRK2-deficient AT2 cells themselves and the mo-Macs they recruited jointly contributed to the recruitment of neutrophils in the process of pulmonary fibrosis. Taken together, these data demonstrated that AT2 cell dysfunction caused by LRRK2 deficiency promoted the recruitment of profibrotic mo-Macs via the CCL2/CCR2 axis, ablation of which attenuated the aggravated pulmonary fibrosis.

Discussion

IPF is associated with disruption of well-coordinated local responses to lung injury, involving epithelial cells, fibroblasts, and infiltrated immune cells (4). AT2 cells act as a critical component in respiratory barrier in regulating pulmonary immune system to protect the lungs from injury (5). In this study, we identified LRRK2 as a pivotal molecule in AT2-coordinated pulmonary responses in the context of BIPF. Our results provided clear evidence that LRRK2 restrained progressive pulmonary fibrosis by preventing AT2 cell dysfunction and the subsequent CCL2/CCR2 axis–dependent macrophage-mediated profibrotic responses (*SI Appendix*, Fig. S13). Our study therefore revealed a crucial role of LRRK2 in orchestrating the innate immune responses and the pulmonary tissue injury and dissected an underlying mechanism for LRRK2-mediated protection from BIPF in vivo.

LRRK2 plays important roles in innate immune responses during infectious and inflammatory diseases in human and mice (9, 13, 16). Given its high abundance in lung, it is desirable to uncover its potential functions in lung homeostasis or diseases. As increasing numbers of studies have reported the regulatory role of LRRK2 in macrophage function (9, 37), we initially expected that the absence of LRRK2 promoted the progression of pulmonary fibrosis in a macrophage-intrinsic manner. Unexpectedly, the results from reciprocal BM transplantation experiments indicated that LRRK2 deficiency in nonhematopoietic cells served as the major contributor to the enhanced sensitivity to BIPF. LRRK2 deficiency in the nonhematopoietic compartment created a profibrotic lung microenvironment that facilitated the recruitment and profibrotic polarization of mo-Macs. At the meantime, considerable production of neutrophil chemokine CXCL1 by the recruited mo-Macs also contributed to the recruitment of neutrophils into the lung of bleomycin-treated *Lrrk2*$^{-/-}$ mice. Furthermore, we speculated that insufficient infiltration of B cells caused by LRRK2 deficiency could also contribute to the markedly elevated accumulation of neutrophils via interrupting the efficient clearance of neutrophils (55). Thus, our results demonstrated that LRRK2 expressed in nonhematopoietic cells was critical for the coordinated immune responses to protect the host from bleomycin-elicited pulmonary fibrosis.

Among the resident nonhematopoietic compartment in lung, AT2 cells play a central role in the IPF pathogenesis because their dysfunction and repetitive cell injury are the actual causes of IPF initiation (56). LRRK2 is predominantly expressed in AT2 cells under homeostatic conditions, an accumulation of enlarged lamellar bodies in AT2 cells of *Lrrk2*$^{-/-}$ mice observed in our and previous studies (20, 21) clearly demonstrated the essential role of LRRK2 in AT2 cell homeostasis. Enlarged lamellar bodies accumulated in AT2 cells were also observed in patients with Hermansky-Pudlak syndrome complicated by pulmonary fibrosis (57), but the direct relationship between enlarged lamellar bodies and pulmonary fibrosis remains unclear. Although no spontaneous lung injury or fibrosis were observed in LRRK2-deficient mice at steady state, disturbed AT2 cell homeostasis after LRRK2 deletion might have great potential to confer the vulnerability to internal and external environment stimuli and trigger more severe lung immune responses.

In this study, we found that the expression of LRRK2 displayed a dramatic decrease in AT2 cells from IPF patients and bleomycin-treated mice, and this result prompted us to focus on the role of LRRK2 in profibrotic responses in this epithelial cell type. LRRK2 is reported to be involved in the induction of autophagic process and silencing endogenous LRRK2 reduced the autophagic capacity in macrophages and microglial (10). Defective autophagy of AT2 cells has been reported to contribute to the progression of pulmonary fibrosis (41). We found that LRRK2 deficiency led to substantially impaired autophagic process in AT2 cells, as evidenced by increased accumulation of p62 and defective formation of autophagic vacuoles, after bleomycin instillation. As a protein with multiple functional domains, LRRK2 can regulate autophagy via different signaling pathways (58). Among the various signaling pathways we examined, including ERK, JNK, mTOR, and Wnt/β-Catenin signaling pathways, only the activation of ERK signaling was significantly impaired in AT2 cells of both saline- and bleomycin-treated *Lrrk2*$^{-/-}$ mice. LRRK2 was reported to be capable of triggering the up-regulation of autophagy by activating the ERK signaling pathway (46). Therefore, the impaired activation of ERK signaling might serve as the major contributor to autophagic dysfunction. As another MAPK family member that can be positively regulated by LRRK2, JNK signaling has been reported as a potential positive regulator of autophagy (47, 59). The decreased activation of JNK signaling in AT2 cells of LRRK2-deficient mice with pulmonary fibrosis might jointly mediate the autophagy impairment. In addition, our findings of enhanced AT2

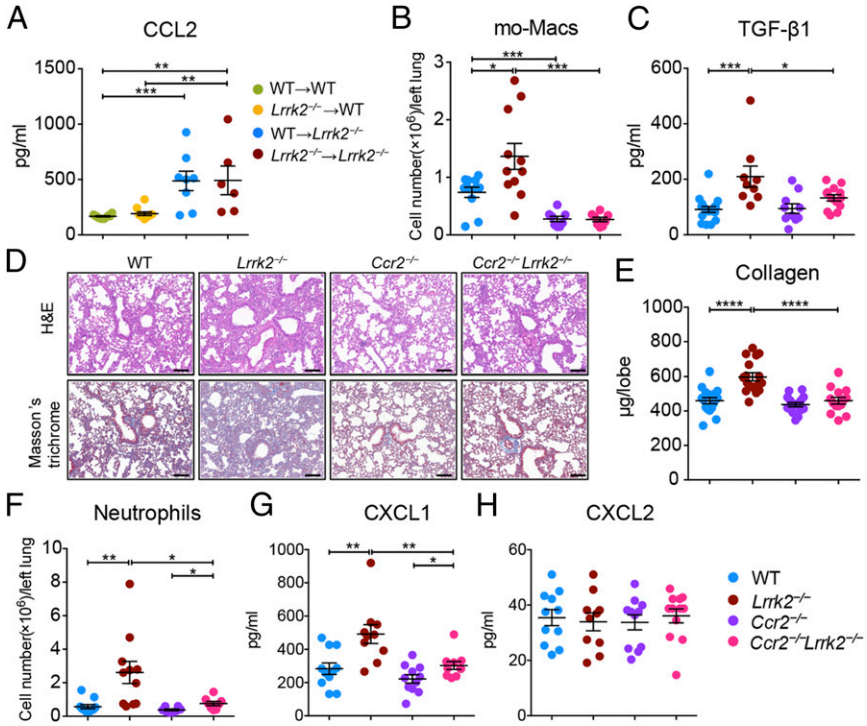

Fig. 7. The enhanced recruitment of mo-Macs and aberrant profibrotic responses were CCL2/CCR2 dependent in LRRK2-deficient mice. (*A*) ELISA analysis of CCL2 concentration in BALF collected from indicated BM chimeric mice treated with 1.5 mg/kg bleomycin for 7 d (n = 6 to 10 mice per group). (*B–H*) WT, *Lrrk2*$^{-/-}$, *Ccr2*$^{-/-}$, and *Ccr2*$^{-/-}$*Lrrk2*$^{-/-}$ mice were treated with 1.5 mg/kg bleomycin for 7 d, and BALF and lung tissues were harvested at day 7 for the following analyses. (*B*) Numbers of mo-Macs in lung tissues were quantified by flow cytometry (n = 8 to 11 mice per group). (*C*) TGF-β1 expression in BALF was quantified by ELISA analysis (n = 9 to 17 mice per group). (*D*) Representative images of H&E and Masson's trichrome staining of lung tissue sections. (Scale bars: 100 μm.) (*E*) Quantification of collagen content in lung homogenates using the Sircol Assay (n = 14 to 17 mice per group). (*F*) Numbers of neutrophils in lung tissues were quantified by flow cytometry (n = 8 to 11 mice per group). (*G* and *H*) ELISA analysis of neutrophil chemoattractant (*G*) CXCL1 and (*H*) CXCL2 levels in BALF (n = 10 to 11 mice per group). Data are shown as mean ± SEM and are integrated from two to three independent experiments. *P < 0.05, **P < 0.01, ***P < 0.001, ****P < 0.0001, two-tailed Student's t test.

cellular senescence in bleomycin-treated LRRK2-deficient mice are of particular interest because epithelial cell senescence has been regarded as one of the hallmarks of pulmonary fibrosis (51). It has been reported that RIPK3 up-regulation promoted lung and kidney fibrosis in either a mixed lineage kinase domain like pseudokinase (MLKL)-mediated necroptosis dependent or independent manner (19, 60). On the contrary, our study revealed that LRRK2 (RIPK7), as another important member of the RIPK family, was indispensable for preventing AT2 cell dysfunction and hence is essential for protecting against bleomycin-mediated pulmonary fibrosis. To date, the regulatory factors upstream of LRRK2 remain elusive. The potential factors including but not limited to transcription factors and noncoding RNAs probably involved in the transcriptional and posttranscriptional regulation of LRRK2 expression require further investigation.

AT2 cells act as the first responders to injury and are essential for the initiation and orchestration of immune responses through recruitment and activation of profibrotic immune cells in the pathogenesis of IPF (6). Moreover, the importance of crosstalk between AT2 cells and macrophages via CCL2/CCR2 axis in exacerbating fibrotic susceptibility has been reported in mouse models of Hermansky-Pudlak syndrome (61). In line with this finding, we observed that the increased numbers of lung-infiltrating mo-Macs were closely correlated with the excessive production of CCL2 by dysfunctional AT2 cells and altered lung environments in *Lrrk2*$^{-/-}$ mice during the course of BIPF. Although the precise underlying mechanisms require further investigation, we speculated that the elevated protein level of IL-13 in lung of bleomycin-injured *Lrrk2*$^{-/-}$ mice might promote the profibrotic polarization of mo-Macs. As LRRK2 has been reported to be a negative regulator of the transcription factor NFAT1, which could drive the transcription of the *Il13* gene (9, 62), the elevated expression level of IL-13 in *Lrrk2*$^{-/-}$ mice probably attributed to the overactivation of NFAT1 signaling. The accumulation of AAMs has been observed in human and murine fibrotic lungs and their canonical function includes the production of TGF-β and other profibrotic mediators, resulting in aggravated fibrogenesis (6). Moreover, TGF-β has been identified as the key factor for inducing fibroblast activation and differentiation into myofibroblasts, which function as effector cells through producing α-SMA and secreting collagen during the progression of tissue fibrosis (63). Several lines of evidence, including BM transplantation experiments and in vitro activation of isolated fibroblasts, collectively supported that the excessive production of TGF-β and subsequent accumulation of activated collagen-secreting myofibroblasts in *Lrrk2*$^{-/-}$ mice were dependent on the recruitment and profibrotic polarization of mo-Macs. Thus, these results elucidated that the loss of LRRK2 in AT2 cells disrupted the coordinated interaction between pulmonary microenvironment and immune cells during fibrotic progression and blocking the abnormal interactions may be beneficial for the treatment of IPF.

In summary, our study unravels a mechanism by which LRRK2 prevents AT2 cell dysfunction to restrain profibrotic responses during the progression of pulmonary fibrosis. Our study convincingly highlights the biological functions of LRRK2 in the maintenance of lung homeostasis and the pathogenesis of fibrotic lung disease, thereby providing potential targets for designing clinical therapeutic strategies.

Materials and Methods

Mice. All mice used in this study were on a C57BL/6 background. *Lrrk2*$^{-/-}$ mice (9) were a kind gift from Zhihua Liu (Tsinghua University, Beijing, China). *Ccr2*$^{-/-}$ mice (JAX stock #017586) (64) were purchased from The Jackson Laboratory. *Lrrk2*$^{-/-}$ mice were crossed to *Ccr2*$^{-/-}$ mice to obtain *Ccr2*$^{-/-}$*Lrrk2*$^{-/-}$ mice. All mice, including WT, were bred and maintained in a specific pathogen-free animal facility at Tsinghua University. The mice were maintained on a 12/12-h light/dark cycle at 22 to 26 °C with sterile pellet food and water ad libitum. All animal procedures were under the approval of the Institutional Animal Care and Use Committee at Tsinghua University.

Models of BIPF. Age-matched male mice between 6 and 8 wk of age (22 to 25 g) were used for induction of BIPF. In brief, mice were anesthetized with 1% sodium pentobarbital via intraperitoneal injection and then treated with 1.2 or 1.5 mg/kg of bleomycin (Selleck) in 40 μL saline or saline alone via intratracheal injection. Body weight change was measured daily, and mice with more than 30% body weight loss were considered dead and killed.

Lung Cell Isolation and Flow Cytometry. For flow cytometry analysis, mouse lung tissues were collected and digested with Collagenase 1A (0.5 mg/mL, Sigma) and DNase I (0.05 mg/mL, Roche) in Hank's Balanced Salt Solution (HBSS) for 60 min at 37 °C with several interval vortexes. Cell suspensions were filtrated through a 70-μm cell strainer, and erythrocytes were removed by using homemade red cell removal buffer (0.168M NH_4Cl). Lung cell suspensions were incubated with homemade antibody against CD16/32 to block nonspecific binding and then stained with fluorochrome-conjugated monoclonal antibodies against CD45, CD11c, Siglec-F, F4/80, MHC-II, Ly6G, CD11b, CD19, CD3ε, CD4, and CD8. Cells were analyzed on the LSR Fortessa instrument (Becton Dickinson), and data were analyzed with FlowJo X software (TreeStar). For isolating mo-Macs and AT2 cells simultaneously, mouse lung lobes were digested with Collagenase 1A (0.5 mg/mL, Sigma), Dispase II (0.1%, Roche), and DNase I (0.05 mg/mL, Roche) in HBSS for 60 min at 37 °C with several interval vortexes. For isolating AT2 cells alone, mouse lungs were digested by Dispase II (0.25% in DMEM/F12, Roche) and DNase I (0.05 mg/mL in DMEM/F12, Roche) as previously described (65). Lung cell suspensions were incubated with purified antibodies against CD45, CD31, CD16/32, and CD24 to enrich the $CD45^-CD31^-CD16/32^-CD24^-$ cells by immunomagnetic bead depletion for subsequent cell sorting. Cell sorting was performed with a FACS Aria III cell sorter (Becton Dickinson) for subsequent experiments. Lung mo-Macs were defined as $CD45^+Siglec\text{-}F^-Ly6G^-CD11b^+F4/80^+$ cells, and lung AT2 cells were defined as $CD45^-CD31^-Podoplanin^-CD24^-EpCAM^+$ cells. Antibodies are listed in the *SI Appendix*, Table S1.

BM Chimeric Mice, Lung Histopathological Analysis, Enzyme Linked Immunosorbent Assay (ELISA), Sircol Assay, qRT-PCR, and Western Blot Analysis. Procedures are detailed in *SI Appendix, Materials and Methods*.

Statistical Analysis. Analysis of all data was done with unpaired two-tailed Student's *t* test or two-way ANOVA followed by Bonferroni's multiple comparisons test indicated in the figure legends (Prism, GraphPad Software). $P < 0.05$ was considered significant.

Data Availability. All study data are included in the article and/or *SI Appendix*.

ACKNOWLEDGMENTS. We thank Prof. Zhihua Liu (Institute for Immunology, School of Medicine, Tsinghua University) for providing *Lrrk2*$^{-/-}$ mice on a C57BL/6 background and valuable advice on the project. We are grateful for the support provided by the animal core facility at Tsinghua University. This research was supported by the Ministry of Science and Technology of China (National Key Research Project 2019YFA0508502 to L.W.), the National Natural Science Foundation of China (Grants 91642207 and 31991174 to L.W., 81971476 to J.Z., 81801641 to J.L., and 31725010 and 31821003 to X.H.), and Tsinghua-Peking Center for Life Sciences (to L.W., X.H., and J.L.).

1. H. A. Chapman, Disorders of lung matrix remodeling. *J. Clin. Invest.* **113**, 148–157 (2004).
2. A. Günther *et al.*, Unravelling the progressive pathophysiology of idiopathic pulmonary fibrosis. *Eur. Respir. Rev.* **21**, 152–160 (2012).
3. W. A. Wuyts *et al.*, The pathogenesis of pulmonary fibrosis: A moving target. *Eur. Respir. J.* **41**, 1207–1218 (2013).
4. T. A. Wynn, Integrating mechanisms of pulmonary fibrosis. *J. Exp. Med.* **208**, 1339–1350 (2011).
5. J. A. Whitsett, T. Alenghat, Respiratory epithelial cells orchestrate pulmonary innate immunity. *Nat. Immunol.* **16**, 27–35 (2015).
6. S. Jia, K. K. Kim, "The function of epithelial cells in pulmonary fibrosis" in *Lung Epithelial Biology in the Pathogenesis of Pulmonary Disease*, V. K. Sidhaye, M. Koval, Eds. (Elsevier Inc., Cambridge, MA, 2017), pp. 103–131.
7. S. Gordon, Alternative activation of macrophages. *Nat. Rev. Immunol.* **3**, 23–35 (2003).
8. M. A. Gibbons *et al.*, Ly6Chi monocytes direct alternatively activated profibrotic macrophage regulation of lung fibrosis. *Am. J. Respir. Crit. Care Med.* **184**, 569–581 (2011).
9. Z. Liu *et al.*, The kinase LRRK2 is a regulator of the transcription factor NFAT that modulates the severity of inflammatory bowel disease. *Nat. Immunol.* **12**, 1063–1070 (2011).
10. J. Schapansky, J. D. Nardozzi, F. Felizia, M. J. LaVoie, Membrane recruitment of endogenous LRRK2 precedes its potent regulation of autophagy. *Hum. Mol. Genet.* **23**, 4201–4214 (2014).
11. P. Gómez-Suaga *et al.*, Leucine-rich repeat kinase 2 regulates autophagy through a calcium-dependent pathway involving NAADP. *Hum. Mol. Genet.* **21**, 511–525 (2012).
12. E. S. Sweet, B. Saunier-Rebori, Z. Yue, R. D. Blitzer, The Parkinson's disease-associated mutation LRRK2-G2019S impairs synaptic plasticity in mouse hippocampus. *J. Neurosci.* **35**, 11190–11195 (2015).
13. Q. Zhang *et al.*, Commensal bacteria direct selective cargo sorting to promote symbiosis. *Nat. Immunol.* **16**, 918–926 (2015).
14. A. Zimprich *et al.*, Mutations in LRRK2 cause autosomal-dominant parkinsonism with pleomorphic pathology. *Neuron* **44**, 601–607 (2004).
15. A. Franke *et al.*, Genome-wide meta-analysis increases to 71 the number of confirmed Crohn's disease susceptibility loci. *Nat. Genet.* **42**, 1118–1125 (2010).
16. F. R. Zhang *et al.*, Genomewide association study of leprosy. *N. Engl. J. Med.* **361**, 2609–2618 (2009).
17. F. Humphries, S. Yang, B. Wang, P. N. Moynagh, RIP kinases: Key decision makers in cell death and innate immunity. *Cell Death Differ.* **22**, 225–236 (2015).
18. K. Shimada *et al.*, The NOD/RIP2 pathway is essential for host defenses against *Chlamydophila pneumoniae* lung infection. *PLoS Pathog.* **5**, e1000379 (2009).
19. J. M. Lee *et al.*, Involvement of alveolar epithelial cell necroptosis in idiopathic pulmonary fibrosis pathogenesis. *Am. J. Respir. Cell Mol. Biol.* **59**, 215–224 (2018).
20. R. N. Fuji *et al.*, Effect of selective LRRK2 kinase inhibition on nonhuman primate lung. *Sci. Transl. Med.* **7**, 273ra15 (2015).
21. M. C. Herzig *et al.*, LRRK2 protein levels are determined by kinase function and are crucial for kidney and lung homeostasis in mice. *Hum. Mol. Genet.* **20**, 4209–4223 (2011).
22. A. Moeller, K. Ask, D. Warburton, J. Gauldie, M. Kolb, The bleomycin animal model: A useful tool to investigate treatment options for idiopathic pulmonary fibrosis? *Int. J. Biochem. Cell Biol.* **40**, 362–382 (2008).
23. R. H. Hübner *et al.*, Standardized quantification of pulmonary fibrosis in histological samples. *Biotechniques* **44**, 507–511, 514–517 (2008).
24. D. J. DePianto *et al.*, Heterogeneous gene expression signatures correspond to distinct lung pathologies and biomarkers of disease severity in idiopathic pulmonary fibrosis. *Thorax* **70**, 48–56 (2015).
25. N. I. Chaudhary, A. Schnapp, J. E. Park, Pharmacologic differentiation of inflammation and fibrosis in the rat bleomycin model. *Am. J. Respir. Crit. Care Med.* **173**, 769–776 (2006).
26. A. V. Misharin, L. Morales-Nebreda, G. M. Mutlu, G. R. S. Budinger, H. Perlman, Flow cytometric analysis of macrophages and dendritic cell subsets in the mouse lung. *Am. J. Respir. Cell Mol. Biol.* **49**, 503–510 (2013).
27. C. Agostini, C. Gurrieri, Chemokine/cytokine cocktail in idiopathic pulmonary fibrosis. *Proc. Am. Thorac. Soc.* **3**, 357–363 (2006).
28. P. J. Sime, Z. Xing, F. L. Graham, K. G. Csaky, J. Gauldie, Adenovector-mediated gene transfer of active transforming growth factor-beta1 induces prolonged severe fibrosis in rat lung. *J. Clin. Invest.* **100**, 768–776 (1997).
29. F. Saito *et al.*, Role of interleukin-6 in bleomycin-induced lung inflammatory changes in mice. *Am. J. Respir. Cell Mol. Biol.* **38**, 566–571 (2008).
30. A. Hancock, L. Armstrong, R. Gama, A. Millar, Production of interleukin 13 by alveolar macrophages from normal and fibrotic lung. *Am. J. Respir. Cell Mol. Biol.* **18**, 60–65 (1998).
31. T. A. Wynn, K. M. Vannella, Macrophages in tissue repair, regeneration, and fibrosis. *Immunity* **44**, 450–462 (2016).
32. O. Desai, J. Winkler, M. Minasyan, E. L. Herzog, The role of immune and inflammatory cells in idiopathic pulmonary fibrosis. *Front. Med. (Lausanne)* **5**, 43 (2018).
33. F. Takahashi *et al.*, Role of osteopontin in the pathogenesis of bleomycin-induced pulmonary fibrosis. *Am. J. Respir. Cell Mol. Biol.* **24**, 264–271 (2001).
34. Y. Li *et al.*, S100A4+ macrophages are necessary for pulmonary fibrosis by activating lung fibroblasts. *Front. Immunol.* **9**, 1776 (2018).
35. W. Zhang *et al.*, S100a4 is secreted by alternatively activated alveolar macrophages and promotes activation of lung fibroblasts in pulmonary fibrosis. *Front. Immunol.* **9**, 1216 (2018).
36. R. Yan, Z. Liu, LRRK2 enhances Nod1/2-mediated inflammatory cytokine production by promoting Rip2 phosphorylation. *Protein Cell* **8**, 55–66 (2017).
37. W. Liu *et al.*, LRRK2 promotes the activation of NLRC4 inflammasome during *Salmonella* Typhimurium infection. *J. Exp. Med.* **214**, 3051–3066 (2017).
38. F. A. Vieira Braga *et al.*, A cellular census of human lungs identifies novel cell states in health and in asthma. *Nat. Med.* **25**, 1153–1163 (2019).
39. M. Huizing, A. Helip-Wooley, W. Westbroek, M. Gunay-Aygun, W. A. Gahl, Disorders of lysosome-related organelle biogenesis: Clinical and molecular genetics. *Annu. Rev. Genomics Hum. Genet.* **9**, 359–386 (2008).
40. Y. Xu *et al.*, Single-cell RNA sequencing identifies diverse roles of epithelial cells in idiopathic pulmonary fibrosis. *JCI Insight* **1**, e90558 (2016).

41. S. Cabrera *et al*., Essential role for the ATG4B protease and autophagy in bleomycin-induced pulmonary fibrosis. *Autophagy* **11**, 670–684 (2015).
42. A. Hawkins *et al*., A non-BRICHOS SFTPC mutant (SP-CI73T) linked to interstitial lung disease promotes a late block in macroautophagy disrupting cellular proteostasis and mitophagy. *Am. J. Physiol. Lung Cell. Mol. Physiol.* **308**, L33–L47 (2015).
43. S. R. Yoshii, N. Mizushima, Monitoring and measuring autophagy. *Int. J. Mol. Sci.* **18**, 1865 (2017).
44. N. Fujita *et al*., The Atg16L complex specifies the site of LC3 lipidation for membrane biogenesis in autophagy. *Mol. Biol. Cell* **19**, 2092–2100 (2008).
45. R. Wallings, C. Manzoni, R. Bandopadhyay, Cellular processes associated with LRRK2 function and dysfunction. *FEBS J.* **282**, 2806–2826 (2015).
46. J. M. Bravo-San Pedro *et al*., The LRRK2 G2019S mutant exacerbates basal autophagy through activation of the MEK/ERK pathway. *Cell. Mol. Life Sci.* **70**, 121–136 (2013).
47. Y. Y. Zhou, Y. Li, W. Q. Jiang, L. F. Zhou, MAPK/JNK signalling: A potential autophagy regulation pathway. *Biosci. Rep.* **35**, 1–10 (2015).
48. K. J. Petherick *et al*., Autolysosomal β-catenin degradation regulates Wnt-autophagy-p62 crosstalk. *EMBO J.* **32**, 1903–1916 (2013).
49. J. Araya *et al*., Insufficient autophagy in idiopathic pulmonary fibrosis. *Am. J. Physiol. Lung Cell. Mol. Physiol.* **304**, L56–L69 (2013).
50. K. Kuwano *et al*., P21Waf1/Cip1/Sdi1 and p53 expression in association with DNA strand breaks in idiopathic pulmonary fibrosis. *Am. J. Respir. Crit. Care Med.* **154**, 477–483 (1996).
51. M. J. Schafer *et al*., Cellular senescence mediates fibrotic pulmonary disease. *Nat. Commun.* **8**, 14532 (2017).
52. T. Tchkonia, Y. Zhu, J. van Deursen, J. Campisi, J. L. Kirkland, Cellular senescence and the senescent secretory phenotype: Therapeutic opportunities. *J. Clin. Invest.* **123**, 966–972 (2013).
53. I. F. Charo, CCR2: From cloning to the creation of knockout mice. *Chem. Immunol.* **72**, 30–41 (1999).
54. T. Okuma *et al*., C-C chemokine receptor 2 (CCR2) deficiency improves bleomycin-induced pulmonary fibrosis by attenuation of both macrophage infiltration and production of macrophage-derived matrix metalloproteinases. *J. Pathol.* **204**, 594–604 (2004).
55. J. H. Kim *et al*., Aged polymorphonuclear leukocytes cause fibrotic interstitial lung disease in the absence of regulation by B cells. *Nat. Immunol.* **19**, 192–201 (2018).
56. M. Selman, T. E. King, A. Pardo; American Thoracic Society; European Respiratory Society; American College of Chest Physicians, Idiopathic pulmonary fibrosis: Prevailing and evolving hypotheses about its pathogenesis and implications for therapy. *Ann. Intern. Med.* **134**, 136–151 (2001).
57. Y. Nakatani *et al*., Interstitial pneumonia in Hermansky-Pudlak syndrome: Significance of florid foamy swelling/degeneration (giant lamellar body degeneration) of type-2 pneumocytes. *Virchows Arch.* **437**, 304–313 (2000).
58. M. Madureira, N. Connor-Robson, R. Wade-Martins, LRRK2: Autophagy and lysosomal activity. *Front. Neurosci.* **14**, 498 (2020).
59. C. J. Gloeckner, A. Schumacher, K. Boldt, M. Ueffing, The Parkinson disease-associated protein kinase LRRK2 exhibits MAPKKK activity and phosphorylates MKK3/6 and MKK4/7, in vitro. *J. Neurochem.* **109**, 959–968 (2009).
60. M. Imamura *et al*., RIPK3 promotes kidney fibrosis via AKT-dependent ATP citrate lyase. *JCI Insight* **3**, e94979 (2018).
61. L. R. Young *et al*., Epithelial-macrophage interactions determine pulmonary fibrosis susceptibility in Hermansky-Pudlak syndrome. *JCI Insight* **1**, e88947 (2016).
62. S. Monticelli, D. C. Solymar, A. Rao, Role of NFAT proteins in IL13 gene transcription in mast cells. *J. Biol. Chem.* **279**, 36210–36218 (2004).
63. J. T. Allen, M. A. Spiteri, Growth factors in idiopathic pulmonary fibrosis: Relative roles. *Respir. Res.* **3**, 13 (2002).
64. N. Saederup *et al*., Selective chemokine receptor usage by central nervous system myeloid cells in CCR2-red fluorescent protein knock-in mice. *PLoS One* **5**, e13693 (2010).
65. M. Gereke *et al*., Flow cytometric isolation of primary murine type II alveolar epithelial cells for functional and molecular studies. *J. Vis. Exp.* **70**, 4322 (2012).